Generalized reduced R-matrix theoretical analysis of the 5He system

Authors: Xu, Han, Ye, Dr. Tao, Prof. Zhenpeng Chen, Guo, Dr. Hairui, Sun, Prof. Weili, Sun, Mr. Zhihao, Fan, Miss Haoyang, Ye, Dr. Tao

Date: 2025-05-29T13:18:16+00:00

Abstract

Based on the Generalized reduced R-matrix theory, the RAC program (R-matrix analysis code) is used to analyze the experimental data of all the nuclear reaction channels related to the 5He system. The current calculations provide accurate and reliable evaluation data, and are in good agreement with the experimental data. In this work, self-consistent for each reaction evaluation data are obtained by multi-channel and multi-energy fitting, in particular, the error propagation theory of Generalized Least Squares is used to give the error of the evaluation data and the covariance matrix of the integral cross section. This R-matrix analysis for the 5He system has the following three features. First, for the first time, the error in the evaluation data of the T(d,n)4He reaction cross section and the covariance matrix of the integral cross section are given. Second, we use only one set of R-matrix parameters to depict the reaction cross section of each reaction channel of the 5He system for the whole energy region in our work. Third, in this evaluation, we have taken into account some of the latest measured experimental data, especially after 2000. The T(d,n)4He reaction cross section at 0.1 MeV and below has been carefully studied. The effect of different energy levels in T(d,n)4He has been analyzed, with the energy levels 3/2+ making a major contribution to cross section, and the role of S-wave and D-wave from 3/2- determines the lean forward trend of the angular distributions at 0.01 MeV - 0.1 MeV.

Full Text

Generalized Reduced R-Matrix Theoretical Analysis of the 5He System

Xu Han,[1] Tao Ye,[2]* Zhen-Peng Chen,[3] Hai-Rui Guo,[2] Wei-Li Sun,[2] Zhi-Hao Sun,[1] and Hao-Yang Fan[1]

[1]Graduate School, China Academy of Engineering Physics, Beijing 100193, China
[2]Institute of Applied Physics and Computational Mathematics, Beijing 100094, China
[3]Tsinghua University, Beijing 100084, China

Based on the Generalized Reduced R-matrix theory, the RAC program (R-matrix analysis code) is used to analyze experimental data from all nuclear reaction channels related to the 5He system. The current calculations provide accurate and reliable evaluated data that show good agreement with experimental measurements. In this work, self-consistent evaluated data for each reaction are obtained through multi-channel, multi-energy fitting. In particular, error propagation theory based on Generalized Least Squares is employed to determine the uncertainties in the evaluated data and the covariance matrix of integral cross sections. This R-matrix analysis of the 5He system has three distinctive features. First, for the first time, uncertainties in the evaluated cross sections for the T(d,n)4He reaction and the covariance matrix of integral cross sections are provided. Second, we use only a single set of R-matrix parameters to describe the reaction cross sections for all channels of the 5He system across the entire energy region. Third, in this evaluation, we have incorporated some of the latest experimental measurements, particularly those published after 2000. The T(d,n)4He reaction cross section at 0.1 MeV and below has been carefully studied. The effects of different energy levels on the T(d,n)4He reaction have been analyzed, with the 3/2+ levels making the dominant contribution to the cross section, while the role of S-wave and P-wave components from the 3/2− state determines the slight forward-peaking trend in the angular distributions between 0.01 and 0.1 MeV.

Keywords: R-matrix theory, Nuclear reaction cross section, Data evaluation, Generalized Least Squares, 5He system

INTRODUCTION

In astrophysical and fusion energy applications, deuteron-induced fusion reactions serve as important sources of energy and neutrons, with the corresponding nuclear reaction cross sections representing core data for these fusion applications. Fusion cross sections are essential for analyzing nuclide abundances in the early universe and for designing fusion reactors [1–5].

Currently, five types of fusion reactions are available to us: the two reaction channels of the DD reaction, the DT reaction, the D^{3}He reaction, and the TT reaction [6].

[FIGURE:1] shows the cross sections for these five reactions. Notably, the DT cross section exhibits a large 5 barn peak due to the presence of the 3/2+ resonance, while the magnitudes of the DD and TT reactions are similar, being two orders of magnitude smaller than DT at energies below 100 keV. The D^{3}He reaction also shows a peak at low energy due to the Li 3/2+ state (a mirror of

the A = 5, He state), but since the charge of ^{3}He is larger than that of T, the Coulomb repulsion between D and ^{3}He is greater, making the peak of the D^{3}He reaction cross section lower than that of the DT reaction.

As the most promising fusion reaction to achieve, precise study of the DT reaction cross section is highly meaningful. Since the 1960s, it has been well established that big bang nucleosynthesis produced light elements through a series of fusion reactions. However, it is less widely recognized that the T(d,n) He reaction was responsible for producing more than 99% of the He generated during the big bang. This He accounts for approximately 25% (by mass) of the primordial elemental composition, with the remainder being primarily ^{1}H. The He produced in this way served as a crucial precursor for the triple-alpha process, which formed ^{12}C and subsequently enabled the synthesis of heavier elements in the universe (the CNO cycle and the proton-proton chain in stars synthesized additional helium). In this sense, a portion of our human existence can be traced back to these fusion reactions.

After decades of development, numerous theoretical and experimental results have been accumulated [6, 19], among which the R-matrix method represents an important approach for nuclear data evaluation. R-matrix theory has been primarily applied to data evaluation for light nuclear systems corresponding to fusion reactions. The introduction of R-matrix theory aims to theoretically describe resonance phenomena in low-energy nuclear reactions, mainly applied to studies of light nuclei, low energies, and nuclear reactions with distinct resonance structures. Wigner and Eisenbud first proposed and developed the general R-matrix theory in 1947 [7]. Starting from the Schrödinger equation of quantum mechanics, the theory employs the important concepts of nuclear grouping space and channel surfaces to make the logarithmic derivatives of the wave functions in the inner and outer regions continuous at the channel surfaces, leading to the R-matrix. By relating the R-matrix to the collision matrix, an equation can be derived that describes the cross sections of resonance phenomena in nuclear reactions.

Concerns about the current evaluation data situation for the 5He system. Among the five major international nuclear databases, only the Evaluated Nuclear Data File (ENDF) provides evaluated data for reaction cross sections in both neutron and deuterium channels, while the other databases provide evaluated data for neutron channels only. According to the ENDF file description, the current data in the ENDF database come from R-matrix analysis of He by G. Hale [8–10] and T(d,n) He Legendre coefficients evaluated by M. Drosg [11]. They use a multi-channel fit to data for n+ He and DT reactions that extends to about 24 MeV excitation energy in the He system. ENDF gives n+ He data only over the original range up to 20 MeV, where it is single-channel scattering. For the DT reaction, ENDF gives integrated cross sections and angular distributions at deuteron energies up to 10 MeV. The energy range for the T(d,n) He reaction has been extended to 30 MeV by matching to Legendre coefficients obtained by M. Drosg. ENDF does not provide uncertainties or covariance ma-

trices in the evaluated data, and the comparison of the evaluation data from this work with ENDF is shown in .

[FIGURE:1] shows the five thermonuclear fusion cross sections versus energy in CM coordinates, with data from ENDF.

Currently, international R-matrix analysis programs for light nuclear data evaluation mainly include the R-matrix Energy Dependent Analysis Code (EDA) [8], an R-matrix analysis program for light nuclear systems developed by Los Alamos National Laboratory (LANL) in the United States. We use the R-matrix Analysis Code (RAC) [12] developed by Prof. Chen Zhenpeng of Tsinghua University, which combines the Generalized Reduced R-matrix theory with covariance analysis theory and has the capability to perform highly automated adjustment of all R-matrix parameters while fitting large amounts of experimental data.

RAC has two main features. First, using Generalized Least Squares (GLS) and error propagation theory, the covariance matrix of experimental data is used to calculate uncertainties and covariance matrices of evaluated values. Second, using the reduced R-matrix theory, it is possible to extend the analyzed energy region to regions of indistinguishable energy levels and to achieve fitting of all available experimental data across major energy regions. The RAC program has been used in various international collaborative projects organized by the International Atomic Energy Agency (IAEA), such as the neutron standard cross section, the R-matrix program for the analysis of charged particles, and the International Neutron Data Evaluation Network. It has also been used to analyze the ^{12}C(n,n+3) and ^{12}C(n,) Be cross sections [13], neutron cross section standards file [14], and has obtained satisfactory results. In recent years, many efforts have been made in China to evaluate nuclear reaction data [23–33]. The final goal is to build a complete and independent database for light nucleus reactions, covering both neutron-induced and charged-particle-induced reactions. As an indispensable component of charged-particle reactions, nuclear fusion reactions require renewed and systematic evaluation to support the development of accurate nuclear data for theoretical research and practical applications.

In this work, the RAC program is used to analyze the He system, focusing on obtaining evaluated cross sections for the neutron incident channel n+ He from 2.53×10 MeV to 46 MeV and the deuteron incident channel D+T from 1×10 MeV to 30 MeV.

This paper provides a brief introduction to the basic reduced R-matrix theory and how to construct covariance matrices using Generalized Least Squares. The three selected reaction channels of He and their experimental data situations are discussed. The integral cross section and differential cross section of T(d,n) He reactions within 0.01 to 0.1 MeV are analyzed in particular. Finally, integral cross sections and important differential cross sections for the remaining reaction channels are shown.

II. THEORETICAL DESCRIPTIONS

A. GENERALIZED REDUCED R-MATRIX THEORY

In Generalized Reduced R-matrix theory, "Generalized" refers to the use of Generalized Least Squares, and "reduced" refers to reduced channels. The basic R-matrix theory is described below, and the role of reduced channels is explained. Generalized Least Squares is described in detail in Chapter C.

The R-matrix theory is well suited for describing resonance phenomena in low-energy nuclear reactions. It allows for adjustment of the contributions from different energy levels to each reaction channel based on experimental data, thereby achieving optimal agreement with observations. For light nuclear systems relevant to fusion reactions, the number of resonance peaks is relatively small. In such cases, the R-matrix method can describe cross section behavior across a wide energy range using only a few energy levels. However, R-matrix theory still has some limitations. One major issue is its inability to treat multi-body reaction channels directly. In the Generalized Reduced R-matrix theory, two approaches are commonly used to address this. The first is to approximate the multi-body reaction as an effective two-body reaction. The second is to treat the multi-body channel as a reduced channel and consider only its overall contribution. This work employs the second method to handle multi-body reactions.

In 1958, a review by Lane and Thomas explained in detail the R-matrix theory of nuclear reactions [15]. In the R-matrix approach, nuclear wave functions are described inside the channel radii by many-body basis functions; outside the channel radii, they are described by a linear combination of two-body Coulomb functions. The reduced width amplitude is defined as the projection of the basis function onto a particular channel configuration at the channel radius. This interpretation assumes that nuclear interactions occurring beyond the channel radius are negligible and that channels involving three or more nuclei are non-essential. In addition, it is assumed that the basis functions used as Hamiltonian eigenfunctions obey a predetermined boundary constraint at the channel radius.

R-matrix theory allows the use of a set of R-matrix parameters to describe experimental data for all two-body nuclear reactions associated with the compound nucleus. For the standard R-matrix model, the R-matrix parameters include the reduced width amplitude ($eV^{1}/^{2}$), the energy level position E (eV), and the channel radius a_c (fm). For the reduced R-matrix model, the R-matrix parameters also include the reduced channel width amplitude Γ_r (eV) in addition to the standard R-matrix parameters, which represent the total contribution of all unconsidered reaction channels in the compound nuclear system. The advantage of considering the reduced channel width amplitude is that the R-matrix analysis can be extended to a higher energy region.

It is assumed that a nuclear reaction system is formed after the collision between the incident particle and the target nucleus. Whether the nuclear reaction sys-

tem is a real compound nuclear system or not, the data from each reaction channel can still be fitted by R-matrix theory. Then the Generalized Reduced R-matrix theory becomes a mathematical tool that can simultaneously fit experimental data from many kinds of nuclear reactions in a nuclear system. The R-matrix parameters obtained by this method are no longer required to have clear physical meaning, as long as they can accurately describe all the experimental data. The Generalized Reduced R-matrix theory has been applied in the U.S. R-matrix analysis program EDA and the RAC used in this work.

B. RAC PROGRAM

[FIGURE:2] shows the flow diagram of the RAC program, illustrating the main input and output files of the RAC program and the parameter optimization flow.

In fact, the reliability of R-matrix analysis results is mainly determined by the degree of conformity between the overall fitted values and the experimental data. If the fitted values and experimental values are consistent within the error range, then the fitted values are reliable. The RAC program uses the GLS method to fit all experimental data of a compound nuclear system simultaneously, and finally obtains a complete set of internally self-consistent evaluated data and covariance matrix. The formulas used to calculate reaction cross sections in the RAC program are all given by Lane and Thomas in Chapter 10 [15].

The elements of the R-matrix used in the RAC program are defined by

$$R_{c'c} = \sum_{\lambda\mu}^{N_1} \gamma_{\lambda c}\gamma_{\mu c'} A_{\lambda\mu} + \sum_{\lambda}^{N_2} \frac{\gamma_{\lambda c'}\gamma_{\lambda c}}{E_\lambda - E} \left(A^{-1}\right)_{\lambda\lambda} + \sum_{c} (S_c(E) - B_c)\gamma_{\lambda c}\gamma_{\mu c} - i\Gamma^r_{\lambda\mu}$$

where c and c' represent different reaction channels, and represent energy levels of a compound nuclear system, c represents the reduced width amplitude, A represents the energy level matrix, E represents energy in the center-of-mass system, Eres represents resonance energy, Sc(E) represents the displacement function, Bc represents the boundary condition, and Γ ̂r represents the total reduced channel width amplitude equal to the contribution of all reduced channels.

The main feature of the Generalized Reduced R-matrix model is the consideration of reduced channels. In a composite nuclear system, as the energy of the composite nucleus increases, reaction channels such as three-body reactions and four-body reactions open up. However, due to the lack of experimental data for most many-body reaction channels, it is not possible to consider them as separate reaction channels in the data evaluation. Reaction channels that cannot be considered separately can be categorized into the reduced channel. The setup of reduced channels helps us extend the data evaluation to higher energies.

C. COVARIANCES, GENERALIZED LEAST SQUARES AND ERROR PROPAGATION LAW

D. Smith [16] presents the professional theory for evaluation of nuclear data and serves as a guide to developing computer programs. Key components of nuclear data evaluation and self-contained methods include: (i) the theory of error distribution and error propagation, (ii) formulas for covariance fitting, (iii) the theory of Generalized Least Squares, (iv) the experimental method for modification of Pearl' s Pertinent Puzzle (PPP), (v) Lette' s criteria for minimizing the effect from occasional "outliers" (constrain the ^{2} value of "outliers," with their maximum contribution typically limited to 9), and (vi) the test for the definiteness of the covariance matrix. These components cannot be ignored if one wants to obtain accurate evaluated values and describe experimental nuclear data objectively and with high precision. The inherent reason for this situation stems from the fact that nuclear measurements invariably encompass long-range, middle-range, and short-range inaccuracies in the observable factors. These inaccuracies are an inevitable part of the process. There is also a correlation between long-range and middle-range errors, establishing a linkage between them.

In the Least Squares formalism, the Conventional Least Squares (CLS) formalism is quite adequate for addressing problems in which the relationships between the observables, y, and the parameters, , to be estimated are inherently linear. The true values, , can never be known exactly, but our procedures aim to provide the best estimates possible for given data. We showed that the procedure could also be used to solve problems that are non-linear, provided that they are first linearized by means of Taylor series expansions. This can be accomplished only if initial estimates of the parameters, , are provided. It is this step within the theory which is rather arbitrary. If we are in a position to make an estimate, , then we ought to be in possession of some information on its uncertainty and, furthermore, that should be taken into consideration in the estimation process.

The GLS formalism is introduced to rectify this deficiency in the CLS formalism. This approach represents an amalgamation of Bayesian methodology with the least-squares condition, and it is clearly the method of choice for solving those non-linear problems where introduction of a priori estimates for the parameters is a requirement. Furthermore, the method can also be used to good advantage for solving inherently linear problems which involve combining a priori information with new data in order to provide a refined solution. For example, we perform a Legendre fit to the differential cross section data. In a first pass, estimates could be made for the Legendre expansion coefficients, , based only on differential data. The CLS technique could be used, since no prior information is available (or required). The integral information could then be introduced in order to derive refined values for the parameters, . If GLS is employed, all of the available uncertainty information will always be properly incorporated into the formalism. In fact, this approach can be used to solve even those problems that could be handled just as well by the simpler method. All that is required

is to introduce any reasonable choice for the prior parameters, with errors large enough so that the new data will be dominant.

The optimization process of the GLS method takes into account the full covariance matrix of the experimental data. In GLS, both statistical errors and systematic errors are considered, which means that the sample no longer satisfies a strictly normal distribution, which is in fact the actual state of our experimental data set. There is no rigorous statistical theory that can prove that the least squares method described above can lead to the generation of an unbiased estimate. But according to classical statistical theory, the "Gauss-Markov" theory [16] shows that under certain conditions GLS can lead to minimum variance estimation.

From the perspective of experimental data, the systematic error of experimental data usually has great uncertainty and complexity. Some experiments are relative measurements, some do not provide systematic errors, and some provide systematic errors that are too large or too small. RAC uses a repeated iterative approach to gradually replace the systematic error of the experimental data with the error of the evaluated value, in order to obtain the most reliable and consistent fit to the data. The analytical process of RAC requires repeated computation of the covariance matrix of the intermediate evaluated values and parameters, which involves a huge amount of computation. The covariance matrix is constructed with reference to D. Smith [16].

In the following, we describe how to construct the covariance matrix with error information taken from the experimental data. Suppose U_i², L_i², M_i², and Y_i² are the total variance, statistical variance, long-range component (LERC) of systematic variance, medium-range (MERC) component of systematic variance, and total systematic variance of the i-th experimental data point, respectively.

The diagonal elements C_jj of the correlation coefficient matrix C are 1 for all. The non-diagonal elements for integral cross sections are

$$C_{ij} = C_{ij}^{L} + C_{ij}^{M}$$

where V , V , ···, V refer to the covariance matrices of the subset data, which are independent of each other. The covariance matrix of calculated values is

$$V = \sum_{k} V_k$$

Here C_{ij}^L refers to the LERC of systematic errors, C_{ij}^M refers to the MERC of systematic errors, and

$$f_{ij} = \exp\left(-\frac{(E_i - E_j)^2}{2W^2}\right)$$

where W is a distribution width parameter, and E_i and E_j stand for energy points of the data.

The non-diagonal elements of C for differential cross sections are

$$C_{ij} = (C_{ij}^{L} + C_{ij}^{M}) \cdot G_{ij}$$

It can be seen from the formulas given above that the correlation coefficient is determined by the total error and systematic error, and a larger systematic error leads to a larger correlation coefficient. The absolute covariance matrix elements of the simulated data can be calculated from the corresponding correlation coefficients as follows:

$$V_{ij} = C_{ij} \cdot U_i \cdot U_j$$

The theoretical formula for error propagation within the R-matrix model fitting is:

$$V_y = DV_pD^{+}$$

The formula adopted for optimizing the R-matrix fitting is

$$\chi^2 = (\theta - \theta_p)^{+} V_p^{-1} (\theta - \theta_p) + (\eta - y)^{+} V^{-1} (\eta - y) \Rightarrow \text{minimum}$$

where refers to all R-matrix parameters, V_p refers to the covariance matrix of the R-matrix parameters, refers to the vector of experimental data, y refers to the vector of calculated values, and V refers to the covariance matrix of the R-matrix parameters.

At the beginning of the analysis, RAC uses ^{2} considering only the second term of Eq. (14) to fit experimental data. After obtaining an appropriate parameter set and its covariance matrix V_p, we then use the optimization formula of GLS, that is, the full Eq. (14) is used to fit experimental data. This group of and V_p is used as the initial values for the next iteration. RAC uses an iterative process to continuously improve the estimated value of and decrease the ^{2} with respect to and with respect to V_p simultaneously. This comes at the cost of using 100 times more CPU time than is required when using CLS or others [12]. The primary benefit of GLS is its capability to apply error propagation theory to accurately generate a covariance matrix for the evaluated data; all matrix elements of the covariance matrix are considered, whereas CLS considers only non-diagonal elements.

5He SYSTEM ANALYSIS PROCESS

A. REACTION CHANNELS

The relationship between fitted data and R-matrix parameters is given by:

$$y - y_0 = D(P - P_0), \quad D_{ki} = \left(\frac{\partial y_k}{\partial P_i}\right)_0$$

Here y refers to the vector of calculated values, D to the sensitivity matrix, and P to the vector of R-matrix parameters. Subscript 0 means optimized original value, k and i are for fitted data and R-matrix parameter subscript respectively. The covariance matrix of parameter P is

$$V_P = (D^+ V^{-1} D)^{-1}$$

Here V refers to the covariance matrix of the data to be fitted, and its inversion matrix can be expressed as follows.

Three reaction channels were retained for this work. The channel radii are shown in . The contribution of all other reaction channels is expressed in terms of the total width of the reduced channel. The initial value of channel radii a_c is given by the equation in the literature:

$$a_c = r_0(A_1^{1/3} + A_2^{1/3})$$

where A and A are the mass numbers of the incident particle and target nuclei, respectively. r is a constant in the range of 1.40–1.50 fm. However, in the actual parameter adjustment process, channel radii a_c are adjustable parameters, and the final result is obtained by fitting the experimental data. The channel radii mainly influence the computation of the Coulomb wave functions. By fixing the channel radii after initial tuning, we retain the original set of Coulomb wave functions, thereby accelerating the overall optimization process.

According to the classification of incident particles, the evaluated data of the 5He system are divided into data for the neutron incident reaction channel (n+ He reaction) and data for the deuteron incident reaction channel (DT reaction). The nuclear reaction channels for neutron incident include: He(n,tot), He(n,el), He(n,d)T, He(n,np)T, and the nuclear reaction channels for deuteron incident include: T(d,n) He, T(d,el), T(d,n) He*, where multiple reaction channels are inverse to each other. There are also deuterium-capture reaction channels with very small reaction cross sections. Since both the multi-body reaction and deuterium-capture cross sections are small compared to the main reaction channels for major neutron and deuterium incidence, the above-mentioned reaction channels are not considered in this work.

In the calculations of R-matrix theory, the computational amount is approximately proportional to the cube of the number of reaction channels. If the incident particle energy is high enough and the compound nuclear system involves many two-body reaction channels and multi-body reaction channels, the number of R-matrix parameters and the computational amount can be significantly reduced by using the reduced channel width amplitude. The reduced channel width amplitude is usually used to replace the contribution of two-body and multi-body reaction channels without experimental data.

In this work, due to the lack of experimental data on multi-body reaction channels such as He(n,2np)D, T(d,2np)D and so on, the contributions of these reaction channels are uniformly replaced by the reduced channel width amplitude. From the literature of D.R. Tilley [17], in the deuterium and tritium exit channel, the deuterium has a high probability of breaking up into a proton and a neutron. Therefore, the reaction channel He(n,np)T is also considered in this work. However, due to the lack of experimental data for this reaction channel, we use the reaction T(d,n) He* with deuteron incidence in ENDF/B-VIII.0 as the inverse reaction channel for this reaction, and calculate the cross section of the neutron incidence channel by the detailed balance principle in the RAC program. For He(n,2n)^{3}He, the two-neutron emission cross section is not present in any of the evaluated nuclear data libraries or experimental data libraries, except for the special library for activation EAF-2010 [18]. The cross sections from this library were adopted, but due to the extremely small cross section of this reaction channel, we temporarily treat its contribution as a background in the program calculations.

B. USE OF EXPERIMENTAL DATA

A more comprehensive collection of experimental data on nuclear reaction cross sections is contained in the EXFOR database [19]. This work refers to almost all experimental data for He+n and T+d in EXFOR. The use of experimental data is shown in .

When using the RAC program to optimize the R-matrix parameters based on experimental data, obvious "odd points" in the experimental data need to be excluded, and then the various experimental data need to be normalized if necessary, with the aim of preventing them from interfering with the optimization of the program and causing the R-matrix parameters to fall into erroneous positions in the high-dimensional space.

IV. ANALYSIS AND DISCUSSION OF RESULTS

A. LOW ENERGY CROSS SECTION FOR T(d,n)4He

The deuterium-tritium fusion reaction cross section is the most important reaction cross section of the 5He system, dominated at low energies by a J $= 3/2+$ resonance. It is this 3/2+ state that makes the cross section of the DT reaction

larger than other fusion reactions in the thermonuclear fusion energy region. For reactor applications, the cross section data within the thermonuclear fusion energy region up to 0.1 MeV are of greatest importance. Since the T(d,n) He reaction cross section below 0.01 MeV is extremely small, the low-energy T(d,n) He reaction cross section we discuss below is mainly for 0.01 MeV–0.1 MeV. In this energy range, the T(d,n) He reaction has only experimental data for the integral cross section at the peak. There is a lack of experimental data on the differential cross section, which creates considerable difficulty in obtaining evaluated data, especially for the low-energy differential cross section.

Theoretically, the differential cross section of the T(d,n) He reaction below 0.1 MeV is very close to isotropic, and we adjusted the isotropic distribution to have a slight forward tilt and used this as an initial value. After several iterations, the initial value is replaced by the program' s calculated value, and its final calculated value is determined by fitting the entire set of experimental data. Without adding reference data when the initial fit is in progress, it would leave too much freedom for adjusting parameters, and it is highly possible that the low-energy differential cross section data would change irregularly.

Since the R-matrix analysis for the 5He system is a systematic evaluation, for the differential cross section of the T(d,n) He reaction at low energies, not only will the experimental data at that location have a constraining effect on the evaluation results, but experimental data in other energy ranges of other reaction channels will also affect the evaluation results. In particular, the differential cross section of the neutron reaction channel He(n,el) around 22 MeV, and the differential cross section data of the T(d,n) He reaction obtained only on the basis of the results of ENDF are not objective. For the objectivity of the evaluation work, the ENDF differential cross section data for the low-energy T(d,n) He reaction in the original reference data were replaced using the calculated values of the current RAC program when the fitting of the full system was almost complete.

According to the calculated value of the low-energy differential cross section of the T(d,n) He reaction and the experimental data of other reaction channels, the evaluated differential cross section data of the T(d,n) He reaction can be obtained relatively objectively in this work. Because this work employs covariance fitting, its main role is to provide uncertainties in the T(d,n) He reaction evaluated data, which is not given by ENDF.

We finally obtained the evaluated results for both the integral cross section and differential cross section of the T(d,n) He reaction below 0.1 MeV, derived from the existing energy level structure after systematic evaluation of the 5He system.

For the integral cross section, the current results from RAC are in good agreement with ENDF and experimental data, and the energy region below 0.1 MeV is basically consistent with the ENDF results, as shown in [FIGURE:3]. RAC-2024 and RAC-2024(2) are two different schemes in the evaluation process of this work. The integral cross section of this energy region is used as an example

to verify the conformity of the results of two evaluation schemes and to demonstrate the accuracy of the evaluated data. RAC-2024(2) in [FIGURE:3] shows the results of another independent scheme that evaluated the 5He system, and the results of the two schemes are basically the same, which verifies the accuracy of the evaluated data. The error in the integral cross section is around 5‰, and the closer the energy is to the peak, the smaller the error, with an error of 2.45‰ at 0.1 MeV. The errors in the integral cross section between 0.01 MeV and 10 MeV are given as percentages in [FIGURE:4]. Because the T(d,n) He reaction peaks near 0.1 MeV, where experimental data are most abundant, the error is smallest there during error analysis. The errors in other energy regions are larger than near 0.1 MeV, which satisfies the basic requirements of error analysis. The covariance information is shown in [FIGURE:5], where we present the correlation coefficients (CC) of the covariance for the integral cross section from 0.01 to 10 MeV.

For the differential cross section, the results are more sensitive to the energy level structure at this position than the integral cross section, and the present results differ somewhat from ENDF. The energy level structure at this position is mainly constrained by the differential cross section for the T(d,n) He reaction below 0.1 MeV and the differential cross section of the He(n,el) reaction around 22 MeV, while for the integral cross section of the T(d,n) He reaction below 0.1 MeV, the integral cross section around 22 MeV for the He(n,el) and He(n,tot), and the interfering effects of the background play a certain role.

[FIGURE:6] shows the evaluated differential cross sections at 0.01, 0.05, and 0.09 MeV. As can be seen from these figures, the central values of the RAC evaluation results differ somewhat from the ENDF results, with the difference in central values being within 5‰ and the ENDF results being within the error range of the RAC evaluation results. The differential cross section of the T(d,n) He reaction at low energy tends to be essentially isotropic. Detailed differential cross section data from the RAC evaluation can be found in the supplementary file (on pages 6-19).

Here is an individual discussion for the differential cross section at E_d = 0.1 MeV and an explanation of why the low-energy differential cross section is forward-peaking from the perspective of wave decomposition. E_d = 0.1 MeV is basically where the peak is, and it is very important to understand how the differential cross section at 0.1 MeV is constructed. The contributions of different energy levels at the peak are analyzed below. As the analysis of the A = 5 systems progresses, accurate knowledge of the reaction channel T(d,n) He can be expected to contribute to our understanding of the levels of He. The resonance observed at a low energy of E_d = 109 keV is widely recognized as attributable to the J = 3/2+ state in He.

[FIGURE:3] shows T(d,n) He from 0.01 to 0.1 MeV. [FIGURE:5] shows correlation coefficients (multiplied by 1×10) of the covariance for T(d,n) He from 0.01 to 10 MeV. [FIGURE:4] shows the error of the T(d,n) He reaction integral cross section evaluation data given by RAC-2024 at 0.01 to 10 MeV. [FIGURE:6]

shows differential cross sections at 0.01, 0.05, and 0.09 MeV for the T(d,n) He reaction.

In the present study, the angular distribution at the peak E_d = 0.1 MeV is forward-peaking, and the following explains what causes this forward-peaking tendency of the angular distribution at the peak. The angular distribution is energy level dependent. We use Legendre polynomials to decompose the angular distribution at 0.1 MeV. Each Legendre polynomial coefficient reflects the contribution of a specific energy level, with different orders corresponding to different physical effects. The formula used to calculate the angular distribution is shown below:

$$p_i(\mu, E) = \sum_{l=0}^{NL} \frac{2l+1}{4\pi} a_l(E) P_l(\mu)$$

where the P_l are Legendre polynomials with maximum order NL. Note that the angular distribution p_i is normalized by the integral cross section. Only the first 4 terms of the Legendre polynomial were taken, with a defaulting to 1. The other coefficients are shown in (for higher-order fits see the supplementary file on pages 4-5). The Legendre polynomials are calculated as shown in [FIGURE:7].

Decomposing Legendre polynomials for the angular distribution, different l values have different shapes. For example, the S-wave (l=0) is horizontal and has no extremes. The P-wave (l=1) shows a tendency to be a straight line with high left and low right. The D-wave (l=2) is extremely large at 0° and 180° and extremely small at 90°. From and [FIGURE:7], it can be seen that the value of a is much larger than that of a and a , and that the S-wave together with the small contribution of the P-wave has basically constituted the shape of the angular distribution with forward tendency. From the R-matrix energy level parameters, the P-wave at this position is mainly from the 3/2− state.

This problem can also be analyzed in terms of the wave decomposition contribution. All waves are discussed separately, and for each wave its contribution to the angular distribution at that energy is calculated individually, with results shown in [FIGURE:8]. It can be seen that J = 3/2+ makes the main contribution to the angular distribution at that energy point, and the contributions of other waves are much smaller than the contribution of J = 3/2+. However, the contributions of individual waves are almost all 90° symmetric, which cannot explain the phenomenon of angular distribution forward-peaking. From this, it can be recognized that the forward-peaking angular distribution should be formed due to interference between individual waves. The angular distribution of J = 3/2+ at 0.1 MeV is a raised peak, and J = 3/2+ interferes with J = 1/2− as well as J = 3/2− to make the calculated values of the angular distribution larger at small angles and smaller at large angles, with the magnitude of interference between J = 3/2+ and J = 3/2− being larger in comparison to that of J = 1/2−. Interference between J = 3/2+ and J = 5/2+ depresses the

peak of the angular distribution results for J = 3/2+ and improves the results for large and small angles. In summary, the four waves J = 1/2−, J = 3/2+, J = 3/2−, and J = 5/2+ essentially compose the angular distribution at 0.1 MeV, and the result is shown in [FIGURE:9].

[FIGURE:8] shows independent contributions of each wave to the T(d,n) He angular distribution at 0.1 MeV in center-of-mass systems. [FIGURE:7] shows calculations of Legendre functions of different orders for the T(d,n) He angular distribution at 0.1 MeV. [FIGURE:9] shows contributions of the four waves 1/2−, 3/2+, 3/2−, and 5/2+ versus the final result in center-of-mass systems.

B. OTHER REACTION CROSS SECTIONS OF THE 5HE SYSTEM

Due to the excessive amount of data for the evaluation of the 5He system, this section only shows and illustrates the integral cross sections and individual differential cross sections considered in this work. Refer to the supplementary file (including integral cross sections, differential cross sections, and neutron polarization differential cross sections) for detailed information.

[FIGURE:10] and [FIGURE:11] show comparisons of the results of all integral cross sections from this work with experimental data and evaluated data. For neutron incidence channels, ENDF/B-VIII.0 gives evaluated data up to 20 MeV, except for He(n,d)T. For the deuterium incidence channel, ENDF/B-VIII.0 gives evaluated data up to 30 MeV. The results of this work are generally consistent with ENDF/B-VIII.0 within the energy range considered by the ENDF file. ENDF data referenced later are taken from ENDF/B-VIII.0.

It should be mentioned that for the total neutron incident cross section, the present work extends the incident neutron energy up to 46 MeV. As shown in [FIGURE:10] (a) and [FIGURE:11], especially at the second peak caused by the 3/2+ energy level due to T(d,n) He opening around 22 MeV, the RAC results are basically consistent with the experimental data within the error range. According to the work of D. Tilley [17], this energy level corresponds to the first 3/2+ state in the compound nuclear system of He. This indirectly reflects that the level distribution obtained within the RAC framework is generally consistent with the experimentally measured level distribution. Here the experimental data have large errors, so it is not a strong constraint for the optimization of the R-matrix parameters. The level distribution in this energy region is mainly constrained by experimental data of the integral and differential cross sections near the first peak of the T(d,n) He reaction, as well as the differential cross sections of the He(n,el) reaction in the same energy range. Compared to the integrated cross sections, the differential data provide stronger constraints, as differences in the shape of the differential cross sections directly determine which partial waves are involved at a given energy.

The elastic scattering cross section for neutrons is shown in [FIGURE:10] (b). Since other reaction channels of the 5He system are not yet open before 20 MeV, the neutron elastic scattering cross section is completely consistent with

the total neutron cross section in this energy range. This reaction cross section shows a small peak around 22 MeV, as does the total cross section, which again is the contribution of the 3/2+ energy level at this energy. The experimental data for neutron elastic scattering have only 4 energy points, at thermal energy and near 20 MeV, and the results of RAC are consistent with both the ENDF evaluation data and the experimental data within the error range.

The deuteron emission cross section for neutrons is shown in [FIGURE:10] (c). The deuteron emission cross section has a threshold of 22.02 MeV, and only R.E. Shamu [20, 21] measured the cross section at the first peak at 22.2 MeV. The FENDL-3 library references these experimental data. The FENDL-3 library requirement is for all evaluation data to be at least 60 MeV, extrapolating the cross section to 60 MeV by following the trend of the last four measured points on a log-log scale. The extrapolated data were published in FENDL-3.2b. M. Drosg [11] has also calculated results for this reaction channel through detailed-balance calculations. The comparison of RAC with FENDL-3.2b, Drosg' s data, and experimental data is shown in [FIGURE:10] (c). There is a lack of experimental data after the first peak, and since this work is a systematic evaluation of the 5He system, the region lacking experimental data will follow the cross section of the inverse reaction T(d,n) He. This is the reason why RAC results are consistent with Drosg' s results. Following the principle of detailed balance, after the first peak of this reaction, the cross section rises gradually as the energy increases, rather than showing a decreasing trend.

[FIGURE:10] (d) shows the reaction cross section of T(d,n) He*, where He* refers to the first excited state of He. The RAC and ENDF results are in general agreement. We have extrapolated the cross section for this reaction based on the R-matrix parameters of the present work to a maximum energy of 30 MeV. The differential cross section of each reaction channel is basically consistent with the experimental data. It should be mentioned that the differential cross section of neutron elastic scattering around 22 MeV plays a very important role in constraining the low-energy differential cross section of the T(d,n) He reaction. [FIGURE:12] (a) shows the comparison of RAC at 21.85 MeV with experimental data.

It should be noted that for the T(d,el) reaction, we used experimental data that were not included in the ENDF evaluation. The RAC results show good agreement with this experimental data. [FIGURE:12] (b) shows the results of the RAC evaluation at 13.85 MeV in comparison with new experimental data [22].

V. SUMMARY

In this work, based on the Generalized Reduced R-matrix theory, the RAC program is used to simultaneously calculate and analyze all available experimental data about the 5He system. The evaluated values of the main reaction cross sections of the 5He system are obtained after setting reasonable reaction

channels, gradually adding and adjusting suitable R-matrix energy levels, and repeatedly iterating and adjusting the R-matrix parameters. Compared with existing mainstream evaluation databases, the overall agreement is good, and the differences are within the allowable range. At the same time, we combine physical principles or mathematical methods to obtain valid data that can be added to the analysis, expanding the data sources and improving the credibility of the calculated values. In particular, the uncertainty and covariance matrix of the T(d,n) He reaction cross section evaluation are given for the first time.

For the integral cross section, the maximum energy of neutron incidence is generally extended to 46 MeV, and the maximum energy of deuteron incidence is generally extended to 30 MeV, which enlarges the scope of the evaluated data. For the differential cross section, results are given for the four reaction channels He(n,el), He(n,d)T, T(d,n) He, and T(d,el) at different incident energies, which is very broad and basically covers the range of existing experimental data. In particular, the low-energy differential cross section for the T(d,n) He reaction is analyzed in detail, with wave decomposition analysis of the angular distribution at 0.1 MeV using Legendre polynomials. The reason for the forward-peaking of the differential cross section near the peak is given in terms of the contribution of S-wave and P-wave components from the 3/2− state. For error analysis, the uncertainties of the integral cross section and differential cross section of each reaction channel, as well as the covariance of the integral cross sections, are given using generalized least squares and error propagation theory.

In the evaluated data of several reciprocal reactions in the 5He system, the cross section data are precisely matched, which further ensures the reliability of the final evaluated data.

VI. SUPPLEMENTARY INFORMATION

This paper provides a supplementary file containing detailed integral and differential cross sections and corresponding error information.

VII. ACKNOWLEDGEMENTS

We thank the other members of the Nuclear Physics Faculty at the Institute of Applied Physics and Computational Mathematics for their help with this work.

VIII. FUNDING

This work was supported by Science Challenge Project No. TZ20180001.

REFERENCES

[1] Jef Ongena, Yuichi Ogawa., Nuclear fusion: Status report and future prospects. Energy Policy 96, 770-778 (2016). doi: 10.1016/j.enpol.2016.05.037

[2] X.Z. Li, B. Liu, S. Chen et al., Fusion cross-sections for inertial fusion energy. Laser and Particle Beams 22, 469-477 (2004). doi: 10.1017/S026303460404011X

[3] X.Z. Li, Q.M Wei, B. Liu et al., A new simple formula for fusion cross-sections of light nuclei. Nuclear Fusion 48, 125003 (2008). doi: 10.1088/0029-5515/48/12/125003

[4] W.F. Li, N. Wang, F. Jia et al., Particle transfer and fusion cross-section for super-heavy nuclei in dinuclear system. Nuclear and Particle Physics 32, 1143 (2006). doi: 10.1088/0029-5515/48/12/125003

[5] C.L. Jiang, K.E. Rehm, B.B. Back et al., Expectations for 12C and 16O induced fusion cross sections at energies of astrophysical interest. Phys. Rev. C 75, 015803 (2007). doi: 10.1103/PhysRevC.75.015803

[6] M.B. Chadwick, M.W. Paris, G.M. Hale et al., Early Nuclear Fusion Cross-Section Advances 1934–1952 and Comparison to Today' s ENDF Data. Fusion Science and Technology 0, 1–63 (2024). doi: 10.1080/15361055.2023.2297128

[7] E.P. Wigner, L. Eisenbud., Higher Angular Momenta and Long Range Interaction in Resonance Reactions. Phys. Rev. 72, 29–41 (1947). doi: 10.1103/PhysRev.72.29

[8] G.M. Hale, M.W. Paris., Data Covariances from R-Matrix Analyses of Light Nuclei. NUCL DATA SHEETS 123, 165-170 (2015). doi: 10.1016/j.nds.2014.12.029

[9] G.M. Hale, T.L. Talley., Deuteron-induced fusion in various environments. Proc. of the Inter. Conf. on Nuclear Data for Science and Technology (1994). doi: 102493181

[10] G.M. Hale, T.L. Talley., Cross sections and spectra for charged-particle induced reactions. Proc. of the Inter. Conf. on Nuclear Data for Science and Technology (1994). doi: 11197868

[11] M. Drosg., DROSG-2000: Neutron source reactions. Data files with computer codes for 56 monoenergetic neutron source reactions. IAEA (2000). doi: IAEA-NDS-87(rev.5)

[12] Z.P. Chen, Y.Y Sun., A Global Fitting Method with the R-Matrix code RAC. IAEA (2019). doi: 10.61092/iaea.zr3b-121v

[13] J. Liu, Z.Q. Cui, Y.W. Hu et al., 12C(n,n+3) and 12C(n, 0)9Be cross sections in the MeV neutron energy region. PHYS LETT B 842, 137985 (2023). doi: 10.1016/j.physletb.2023.137985

[14] V.G. Pronyaev, S.A. Badikov, Z.P. Chen et al., Status of the International Neutron Cross-Section Standards File. AIP Conf. Proc. 769, 808-815 (2005). doi: 10.1063/1.1945130

[15] A.M. Lane, R.G. Thomas., R-Matrix Theory of Nuclear Reactions. Rev. Mod. Phys. 30, 257-353 (1958). doi: 10.1103/RevModPhys.30.257

[16] D.L. Smith., Probability, statistics, and data uncertainties in nuclear science and technology. American Nuclear Society (1991). ISBN: 0-89448-036-7

[17] D.R. Tilley, C.M. Cheves, J.L. Godwin., Energy levels of light nuclei A=5, 6, 7. NUCL PHYS A 708, 3-163 (2002). doi: 10.1016/S0375-9474(02)00597-3

[18] L.W. Packer., The European Activation File: EAF-2010 biological, clearance and transport libraries. CCFE (2010).

[19] V.V. Zerkin, B. Pritychenko., The experimental nuclear reaction data (exfor): Extended computer database and web retrieval system. NUCL INSTRUM METH A 888, 31-43 (2018). doi: 10.1016/j.nima.2018.01.045

[20] R.E. Shamu, J.G. Jenkin., Neutron-alpha scattering in the 20-MeV range. PHYS REV 135, B99 (1964). doi: 10.1103/PhysRev.135.B99

[21] R.E. Shamu, G.G. Ohlsen, P.G. Young., The He5 States at High Excitation Energies. Physics Letters 4, 286-288 (1963). doi: 10.1016/0031-9163(63)90603-6

[22] B.G. Struzhko., Angular Distribution of Nucleon Pairs in d + t Reaction at the Deutron Energy of 13.85 MeV. Bull.Russian Academy of Sciences - Physics 64, 370 (2000). doi: 20081710

[23] J.S. Zhang., UNF code for fast neutron reaction data calculation, Nucl Sci Eng 142, 207-219 (2002). doi: 10.13182/NSE02-02

[24] Z.G. Ge, R.R Xu, P. Liu., Nuclear Data Evaluation and Chinese Evaluated Nuclear Data Library. Atomic Energy Science and Technology 56, 783-797 (2022). doi: 10.7538/yzk.2022.youxian.0221

[25] T.J. Zu, Y.H. Huang, Q.C. Teng et al., Application of CENDL-3.2 and ENDF/B-VIII.0 on the reactor physics simulation of PWR. ANN NUCL ENERGY 158, 108238 (2021). doi: 10.1016/j.anucene.2021.108238

[26] W.Y. Shu, T.J. Zu, L.Z. Cao et al., Performance of CENDL-3.2 evaluated nuclear data library for the shielding benchmarks. PROG NUCL ENERG 136, 103727 (2021). doi: 10.1016/j.pnucene.2021.103727

[27] J.J. Hu, B. Zhang, Z.W. Zong et al., Verification of CENDL-3.2 nuclear data on VENUS-3 shielding benchmark by ARES transport code. SCI TECHNOL NUCL INS 3, 1-13 (2021). doi: 10.1155/2021/6633366

[28] T.Y. Huang, Z.G. Li, S.H. Jiang et al., Verification of CENDL-3.2 and ENDF/B-VIII.0 evaluated nuclear data library on HTR-10 benchmark. Frontiers in Energy Research 9, 829402 (2022). doi: 10.3389/fenrg.2021.829402

[29] D.J. Cai, Q.C. Liang, T.J. Liu et al., Chinese evaluated nuclear data library, version 2 (CENDL-2). Chinese Journal of Nuclear Science and Engineering 17, 257-265 (1997). doi: 10.1007/978-3-642-58113-7-225

[30] Z.G. Ge, R.R. Xu, H.C. Wu et al., CENDL-3.2: The new version of Chinese general purpose evaluated nuclear data library. EPJ WEB CONF 239, 09001 (2020). doi: 10.1051/epj-conf/202023909001

[31] Y.W. Hu, Y.M. Gledenov, Z.Q. Cui et al., Cross section measurement for the 14N(n, 0,1)11B reactions in the 4.5–11.5 MeV neutron energy region. EUR PHYS J A 60, 51 (2024). doi: 10.1140/epja/s10050-024-01268-9

[32] G.H. Zhang, J.X. Chen, G.Y. Tang et al., Measurement of differential and angle-integrated cross sections of the 6Li(n,t)4He reaction in the MeV neutron energy range. NUCL INSTRUM METH A 566, 615-621 (2006). doi: 10.1016/j.nima.2006.06.064

[33] Y.Y. Ding, Y.B. Nie, Y. Zhang et al., Benchmark experiment on slab 238U with D-T neutrons for validation of evaluated nuclear data. NUCL SCI TECH 35, 29 (2024). doi: 10.1007/s41365-024-01386-5

SUPPLEMENTARY FILE CONTENTS

Integral Cross Section

Figure 1. T(d,n) He from 1×10^{3} to 30 MeV in log-log coordinate. The deuterium-tritium fusion reaction cross section is the most important reaction cross section of the 5He system, dominated at low energies by a JΠ = 3/2+ resonance. It is this 3/2+ state that makes the cross section of the DT reaction larger than other fusion reactions in the thermonuclear fusion energy region. The experimental data for this reaction are very extensive, basically covering from 1×10^{3} to 30 MeV. The comparison of RAC results with ENDF and experimental data is shown in Fig. 1. The experimental data for V.A. Davidenko are in poor agreement with other experimental and evaluation data, and the results of RAC are in general agreement with most of the experimental data. For energies less than 0.01 MeV, due to the lack of experimental data, we can only say that our results are consistent with ENDF/B-VIII.0.

Figure 2. T(d,n) He* from 4.6 to 30 MeV in linear coordinate. This figure shows the reaction cross section of T(d,n) He* where He* refers to the first excited state of He. The RAC and ENDF results are in general agreement, and we have extrapolated the cross section for this reaction based on the R-matrix parameters of the present work to a maximum energy of 30 MeV. There is no available experimental data for this reaction channel, and this work was evaluated using the ENDF/B-VIII.0 evaluation data as a reference.

Figure 3. He(n,tot) from 1×10^{11} to 46 MeV in linear coordinate. It should be mentioned that for the total neutron incident cross section, the present work extends the incident neutron energy up to 46 MeV. As shown in Fig. 3 and Fig. 4, especially at the second peak caused by the 3/2+ energy level due to T(d,n) He opening around 22 MeV, the RAC results are basically consistent with the experimental data within the error range. For B. Haesner' s experimental data, only a few data points were registered in the EXFOR database; the rest of the data points were obtained by reading the graphs from his article. Here

the experimental data have large errors, so it is not a strong constraint for the optimization of the R-matrix parameters.

Figure 4. He(n,tot) from 21.5 to 23 MeV in linear coordinate. The elastic scattering cross section for neutrons is shown in Fig. 5. Since the other reaction channels of the 5He system are not yet open before 20 MeV, the neutron elastic scattering cross section is completely consistent with the total neutron cross section in this energy range. This reaction cross section shows a small peak around 22 MeV, as does the total cross section, which again is the contribution of the 3/2+ energy level at this energy. The experimental data for neutron elastic scattering have only 4 energy points, at very low energy and near 20 MeV, and the results of RAC are consistent with both the ENDF evaluation data and the experimental data within the error range.

Figure 5. He(n,el) from 1×10^{11} to 25 MeV in linear coordinate. The deuteron emission cross section for neutrons is shown in Fig. 6. The deuteron emission cross section has a threshold of 22.02 MeV, and only R.E. Shamu measured the cross section at the first peak at 22.2 MeV. The FENDL-3 library references these experimental data. The FENDL-3 library requirement is for all evaluation data to be at least 60 MeV, extrapolating the cross section to 60 MeV by following the trend of the last four measured points on a log-log scale. The extrapolated data were published in FENDL-3.2b. M. Drosg has also calculated results for this reaction channel through detailed-balance calculations. There is a lack of experimental data after the first peak, and since this work is a systematic evaluation of the 5He system, the region lacking experimental data will follow the cross section of the inverse reaction T(d,n) He. This is the reason why RAC results are consistent with Drosg' s results. Following the principle of detailed balance, after the first peak of this reaction, the cross section rises gradually as the energy increases, rather than showing a decreasing trend.

Figure 6. He(n,d)T from 22 to 27 MeV in linear coordinate.

Differential Cross Section

1. T(d,n) He The first presentation is a comparison of RAC with experimental data, and the results of RAC are in better agreement with experimental data at different energy points. Comparison plots are shown grouped according to experimental data from different experimenters. The results for RAC with more energy points are shown in the last part of this section.

- T.F. Stratton (1952)
- A. Galonski (1956)
- L. Stewart (1960)
- J.E. Simmons (1968)
- D.K. McDaniels (1972)
- N. Jarmie (1977)
- M. Drosg (1978)
- R. Roy (1981), O.M. Bilaniuk (1964) and T. Sakai (1989)

The prediction of absolute differential cross sections of T(d,n) He at projectile energies above 20 MeV is based on charge symmetry with ^{3}He(d,p) He. The results of RAC are compared here with the cross-sectional data for this reaction channel, and the results show good conformity.

More evaluation data of RAC. This section shows the results of the RAC evaluation from 0.01 MeV–30 MeV, compared with ENDF/B-VIII.0 and some of the experimental data mentioned above.

2. T(d,el) The first presentation is a comparison of RAC with experimental data, and the results of RAC are in better agreement with experimental data at different energy points. Comparison plots are shown grouped according to experimental data from different experimenters. The results for RAC with more energy points are shown in the last part of this section.

- J.C. Allred (1952)
- W.R. Stratton (1952)
- J.E. Brolley Jr. (1960)
- M. Ivanovich (1968)
- B.G. Struzhko (2000)

More evaluation data of RAC. This section shows the results of the RAC evaluation from 0.01 MeV–30 MeV, compared with ENDF/B-VIII.0 and some of the experimental data mentioned above.

3. He(n,el) The first presentation is a comparison of RAC with experimental data, and the results of RAC are in better agreement with experimental data at different energy points. Comparison plots are shown grouped according to experimental data from different experimenters. The results for RAC with more energy points are shown in the last part of this section.

All differential cross sections around 22 MeV for neutron elastic scattering play an important role in constraining the differential T(d,n) He reaction at low energies of 0.01–0.1 MeV. R.E. Shamu, B. Hoop, and three experimental data sets have experimental points around 22 MeV, and the RAC results are in general agreement with them. However, due to the small peak around 22 MeV of the neutron elastic scattering cross section being too narrow, its position is extremely sensitive to the distribution of energy levels, and some of the evaluated results differ from the trend of the experimental data, which may be due to the irrational distribution of energy levels at this energy point and needs to be further improved.

- J.D. Seagrave (1953)
- D.F. Shaw (1955)
- S.M. Austin (1962)
- P.G. Young (1963)
- R.E. Shamu (1964)
- U. Fasoli (1963)

- R. Malaroda (1963)
- B. Hoop Jr. (1966)
- A. Niller (1971)
- D.S. Cramer (1972)

More evaluation data of RAC. This section shows the results of the RAC evaluation from 2.53×10 MeV–30 MeV, compared with ENDF/B-VIII.0 and some of the experimental data mentioned above.

4. He(n,d)T For He(n,d)T, ENDF/B-VIII.0 does not provide evaluation data, and there is also a lack of experimental data. Our results are compared with those of M. Drosg.

- Th. Stammbach (1970)

5. He(n,el)-POL The polarization angular distribution of neutron elastic scattering is very sensitive to the energy level. Some comparisons of RAC results with experimental polarization angular distribution data are shown here to justify the R-matrix energy level distribution.

- J.R. Sawers (1968)
- W.B. Broste (1972)
- P.W. Lisowski (1975)
- H. Krupp (1984)

TABLE 1. Comparison of the final results of this work with ENDF/B-VIII.0, including reaction channels, energy range, and whether uncertainties are provided.

Reaction channel	Energy range (MeV)	Error (Y/N)	Reaction channel	Energy range (MeV)	Error (Y/N)
He(n,tot)	2.53×10 – 46.0	Y	He(n,tot)	1×10 [11]– 20.0	N
He(n,el)	2.53×10 – 46.0	Y	He(n,el)	1×10 [11]– 20.0	N
He(n,d)T	1×10 -30.0	Y	T(d,n) He	1×10 -30.0	N
T(d,n) He	1×10 -30.0	Y	T(d,n) He*	1×10 [2]–10.0	N
T(d,n) He*	1×10 -30.0	Y	T(d,el)	1×10 -10.0	N
T(d,el)	9.60×10 [1]– 14.4	Y			

TABLE 2. Channel radii of reaction channels.

Reaction channel	Channel radii a_c (fm)
He + n	4.5
T + d	3.5
He* + n	4.5

TABLE 3. Experimental data used in the RAC program.

Reaction channel	Cross section type	Energy range (MeV)	Data points	Average [2]
He(n,tot)	total cross section	1.87×10 -40.0	1,100	1.2
He(n,el)	integral cross section	2.53×10 -23.7	850	1.1
He(n,d)T	integral cross section	7.00×10 [3]-16.0	200	1.3
T(d,n) He	integral cross section	1.03×10 [2]-20.0	1,500	1.0
He(n,el)	differential cross section	5.45×10 [1]-23.7	600	1.2
T(d,n) He	differential cross section	1.03×10 [2]-20.0	800	1.1
T(d,el)	differential cross section	9.60×10 [1]-14.4	300	1.0

TABLE 4. Legendre coefficients for differential cross sections at 0.01, 0.05, and 0.1 MeV for T(d,n) He reaction.

E_d (MeV)	CS (mb)	a	a	a
1.732×10	2.808×10	2.203×10	4.312×10	1.370×10[3]
4.614×10	1.688×10	-4.429×10	4.936×10[3]	1.342×10 [3]
-1.849×10	-3.599×10			

Legendre coefficients of the differential cross section of T(d,n) He at 0.01 MeV–0.1 MeV

The current cross sections for each reaction channel need to be given in the standard ENDF-6 format. The Legendre coefficients are given below for the T(d,n) He differential cross section at 0.01 MeV–0.1 MeV as an example. The Legendre coefficients and formulas are shown below and are identical to the calculations in the ENDF-6 Formats Manual. The formula is:

$$\frac{d\sigma}{d\Omega}(E,\theta) = \sigma(E)\sum_{l=0}^{NL} a_l(E)P_l(\cos\theta)$$

where the P_l are Legendre polynomials with maximum order NL. Note that the angular distribution is normalized by the integral cross section.

E (MeV)	a	a	a	a	a	a	a	a	a	a	a	a
1.732E-04	2.808E-04	2.203E-04	1.312E-07	9.635E-08	5.448E-09	7.372E-10	-2.846E-10	-4.596E-10	-1.815E-09	-1.960E-09	-5.883E-09	-6.026E-09
5.448E-05	1.428E-04	2.103E-04	6.709E-08	4.277E-08	1.074E-08	7.284E-10	-2.791E-10	-4.616E-10	-1.815E-09	-1.954E-09	-5.878E-09	-6.026E-09
2.810E-04	2.402E-04	1.959E-04	1.012E-06	1.293E-07	1.704E-08	7.057E-10	-2.694E-10	-4.596E-10	-1.822E-09	-1.954E-09	-5.876E-09	-6.027E-09
7.164E-04	2.780E-04	1.821E-04	2.512E-06	3.951E-07	2.401E-08	6.957E-10	-2.773E-10	-4.629E-10	-1.816E-09	-1.957E-09	-5.883E-09	-6.027E-09
1.370E-03	2.610E-04	1.688E-04	4.429E-06	7.385E-07	3.187E-08	6.543E-10	-2.785E-10	-4.455E-10	-1.822E-09	-1.968E-09	-5.886E-09	-6.028E-09
2.202E-03	2.510E-04	1.555E-04	6.829E-06	1.147E-06	4.133E-08	6.678E-10	-2.731E-10	-4.654E-10	-1.818E-09	-1.964E-09	-5.891E-09	-6.029E-09
3.113E-03	2.435E-04	1.408E-04	9.815E-06	1.610E-06	5.423E-08	6.581E-10	-2.687E-10	-4.667E-10	-1.819E-09	-1.968E-09	-5.895E-09	-6.030E-09
3.957E-03	2.403E-04	1.240E-04	1.354E-05	2.118E-06	7.383E-08	7.496E-10	-3.241E-10	-4.881E-10	-1.784E-09	-2.009E-09	-5.922E-09	-6.011E-09
4.589E-03	2.403E-04	1.040E-04	1.823E-05	2.663E-06	1.055E-07	6.420E-10	-2.479E-10	-4.693E-10	-1.821E-09	-1.975E-09	-5.905E-09	-6.031E-09
4.936E-03	3.402E-04	-1.849E-04	-3.599E-06	8.248E-06	5.381E-07	1.355E-06	-2.974E-08	-7.211E-08	3.533E-08	1.082E-07	7.305E-08	5.022E-07

Note: The supplementary file contains detailed integral and differential cross sections and corresponding error information for all reaction channels analyzed in this work. The complete set of figures and tables referenced in the main text can be found in this supplementary material.

Figures

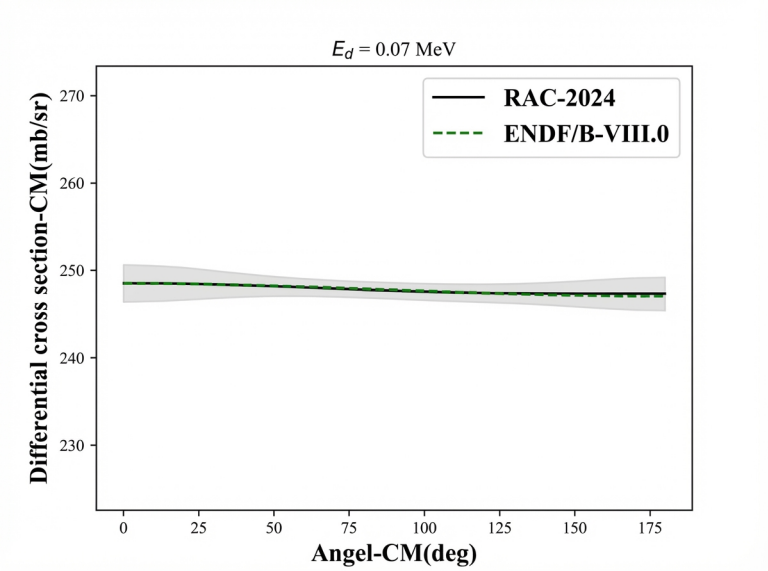

Figure 1: Figure 22

Source: ChinaXiv —Machine translation. Verify with original.

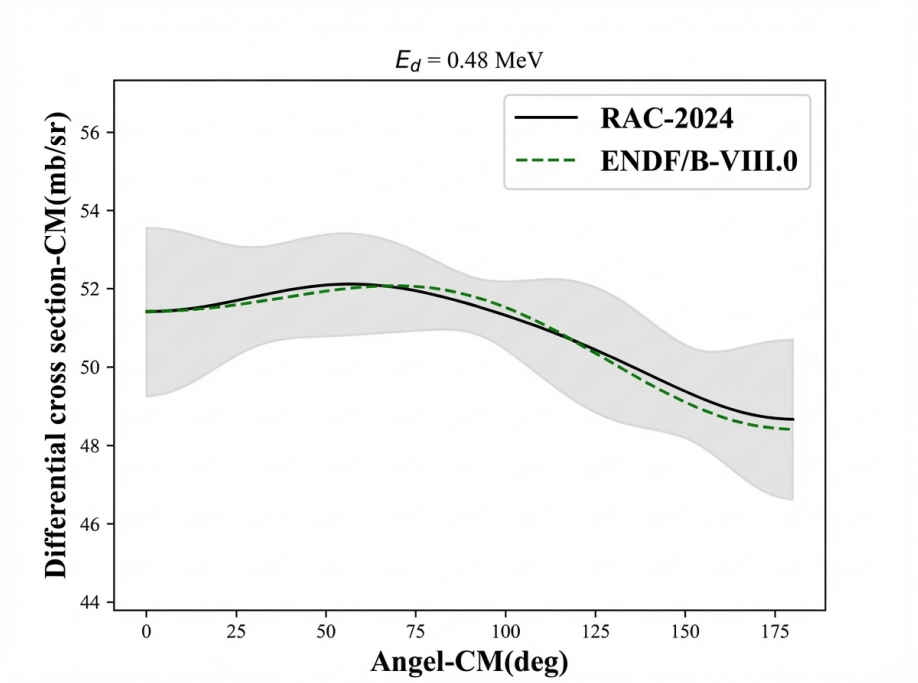

Figure 2: Figure 23

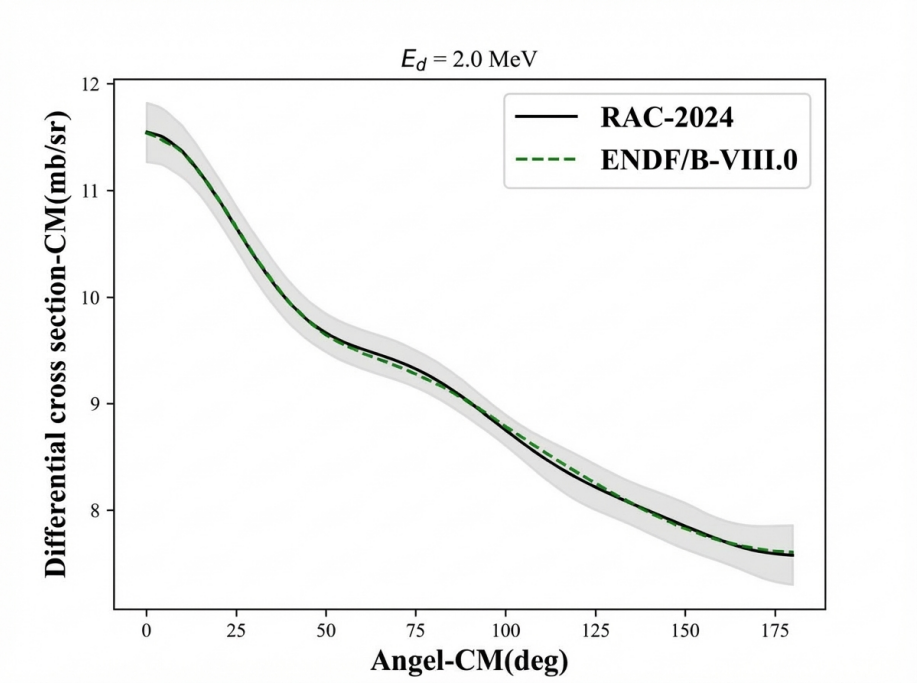

Figure 3: Figure 27

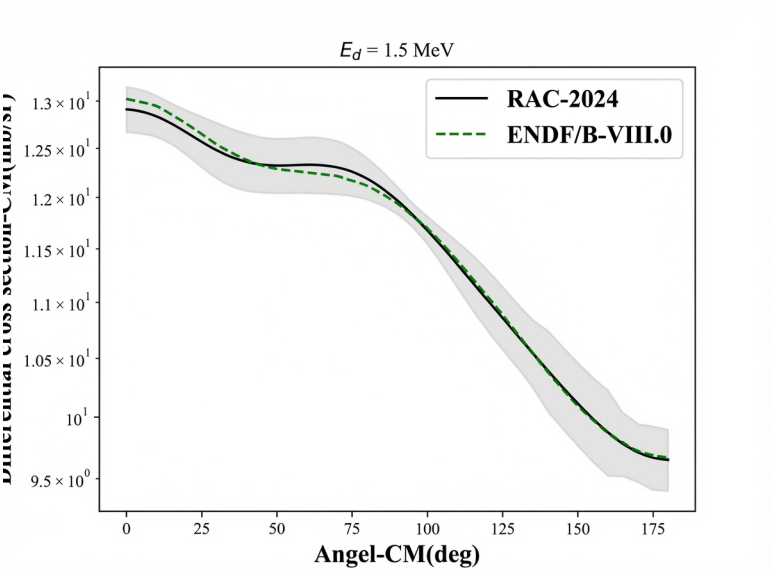

Figure 4: Figure 29

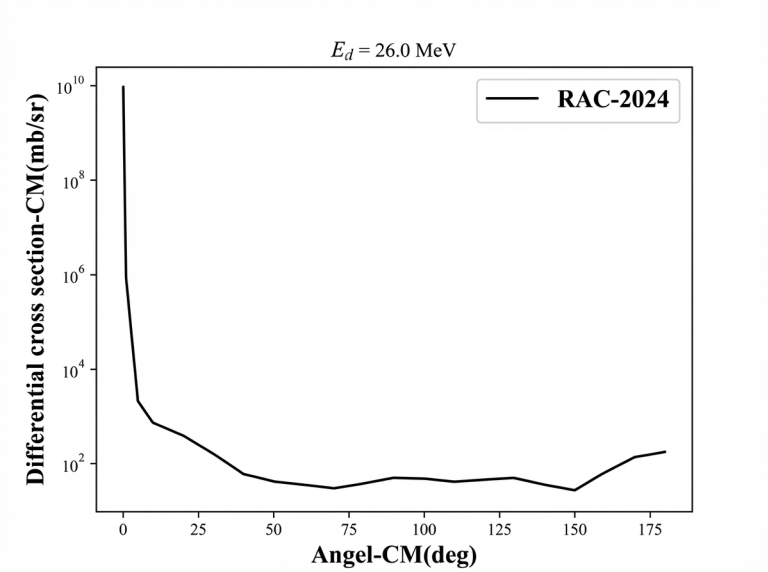

Figure 5: Figure 43

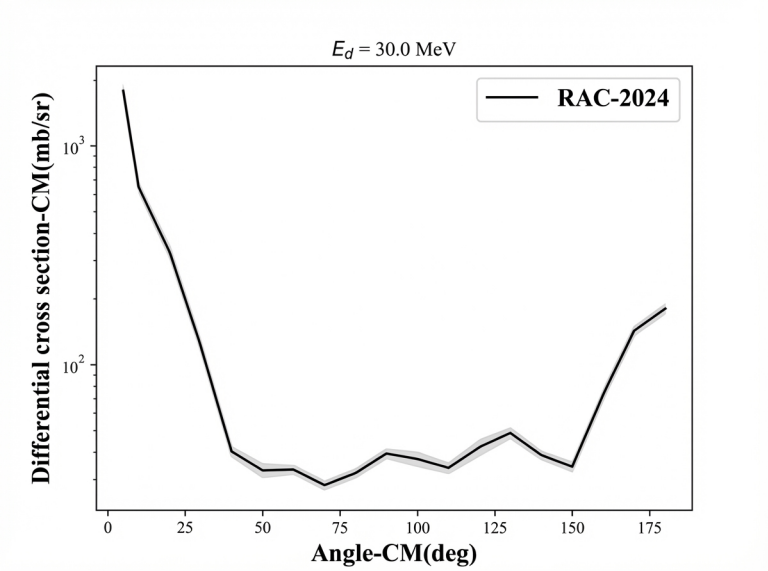

Figure 6: Figure 44

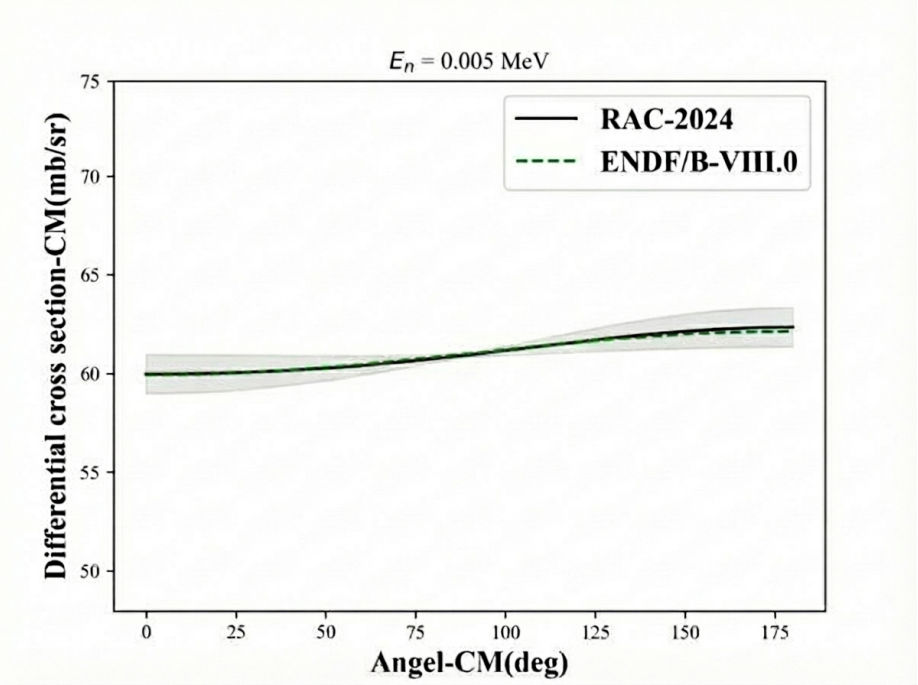

Figure 7: Figure 54

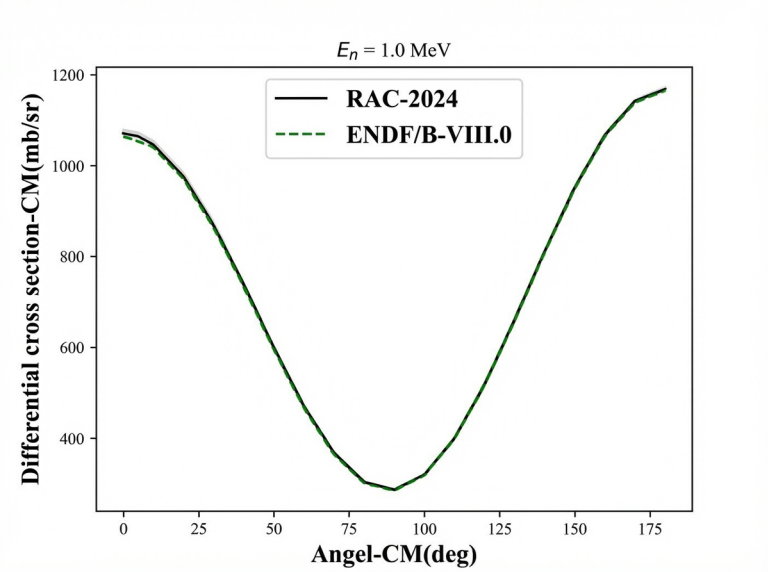

Figure 8: Figure 60

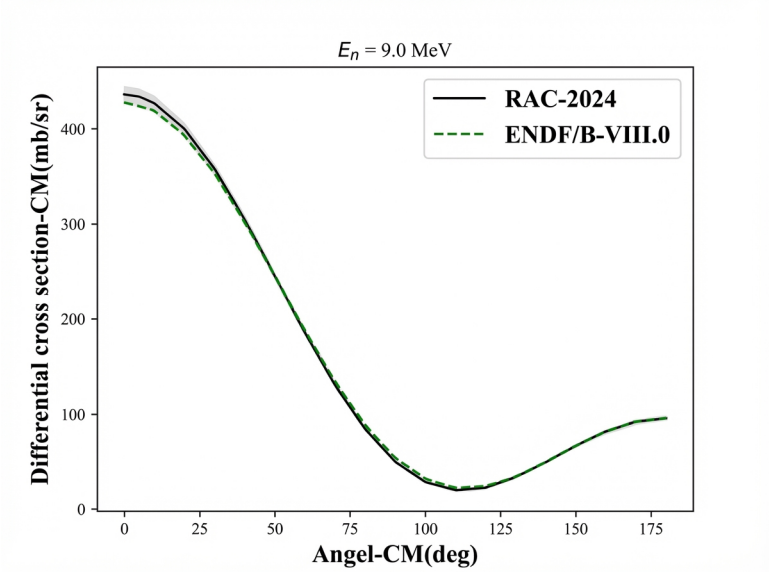

Figure 9: Figure 62

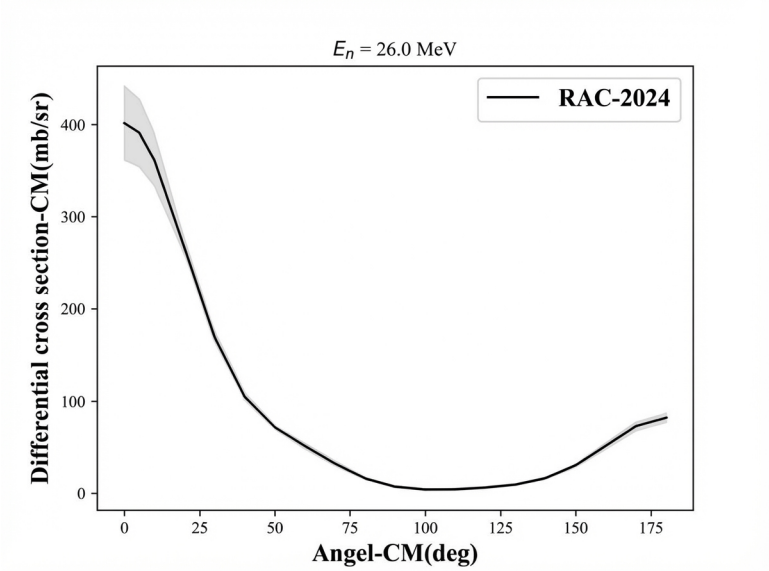

Figure 10: Figure 64

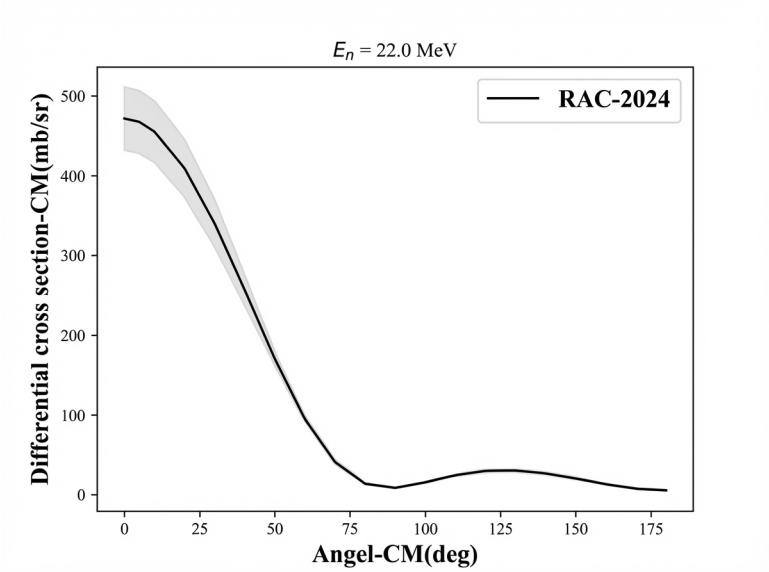

Figure 11: Figure 65

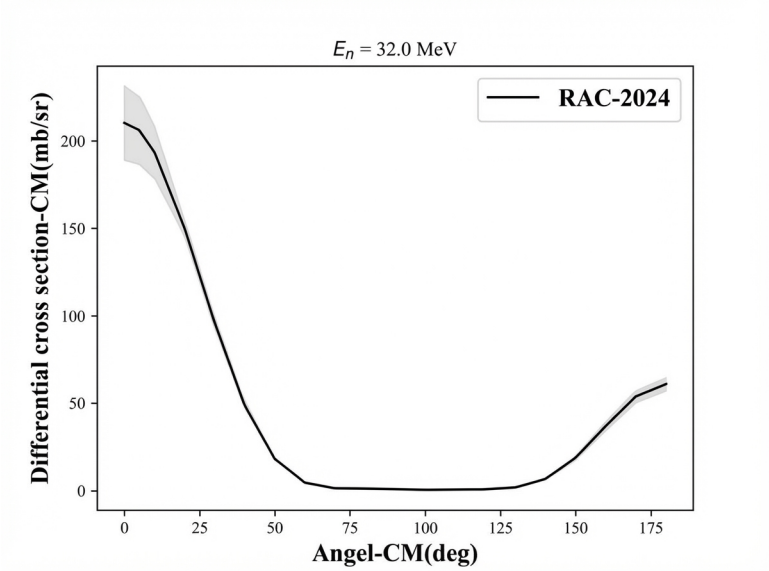

Figure 12: Figure 66